

RKKY interaction in heavily vacant graphene

Alireza Habibi¹ and S. A. Jafari¹

¹*Department of Physics, Sharif University of Technology, Tehran 11155-9161, Iran*

(Dated: July 16, 2018)

Dirac electrons in clean graphene can mediate the interactions between two localized magnetic moments. The functional form of the RKKY interaction in pristine graphene is specified by two main features: (i) an atomic scale oscillatory part determined by a wave vector \vec{Q} connecting the two valleys. Furthermore with doping another longer range oscillation appears which arise from the existence of an extended Fermi surface characterized by a single momentum scale k_F . (ii) R^α decay in large distances where the exponent $\alpha = -3$ is a distinct feature of undoped Dirac sea (with a linear dispersion relation) in two dimensions. In this work, we investigate the effect of a few percent vacancies on the above properties. Depending on the doping level, if the chemical potential lies on the linear part of the density of states, the exponent α remains close to -3 . Otherwise α reduces towards more negative values which means that the combined effect of vacancies and the randomness in their positions makes it harder for the carriers of the medium to mediate the magnetic interaction. Addition of a few percent of vacancies diminishes the atomic scale oscillations of the RKKY interaction signaling the destruction of two-valley structure of the parent graphene material. Surprisingly by allowing the chemical potential to vary, we find that the longer-range oscillations expected to arise from the existence of a k_F scale in the vacant graphene are absent. This may indicate possible non-Fermi liquid behavior by "alloying" graphene with vacancies. The complete absence of oscillations in heavily vacant graphene can be considered an advantage for applications as a uniform sign of the exchange interaction is desirable for magnetic ordering.

PACS numbers: 71.23.-k, 73.22.Pr, 71.55.-i, 71.10.Hf

INTRODUCTION

Two-dimensional nature of graphene, along with the Dirac nature of charge carriers [1] –as contrasted to the Schroedinger nature of the carriers in ordinary conductors – makes graphene a spectacular platform for condensed matter realization of many exciting ideas of low-dimensionality and relativistic physics [2, 3]. Among the properties of interest in materials is the nature of effective interaction between external agents mediated by the carriers of the host materials. An important example of this would be the Ruderman-Kittel-Kasuya-Yosida (RKKY) interaction which is the exchange interaction between two magnetic impurities mediated via the propagators of the host. The RKKY interaction in graphene was studied first by Saremi [4] who found a generic "atomic-scale" oscillatory behavior where the sign of the interaction alternates between the two sub-lattices of the bipartite honeycomb structure. The wave vector characterizing these oscillations is $\vec{Q} = \vec{K}^+ - \vec{K}^-$ where \vec{K}^\pm denote the momenta associated with two Dirac cones. The oscillations decay as R^{-3} in long distances, where the exponent $\alpha = -3$ comes from the linear Dirac cone dispersion in two dimensions. The investigation of Saremi was extended by Sherafati and Satpathy in two directions. First for the undoped graphene they extended the results to a model of full π -bands [5]. Secondly for the low-energy Dirac cone model, they considered the effect of non-zero doping [6], and as in ordinary two-dimensional conductors additional k_F -related oscillations with a R^{-2} decay at large distances appeared. Such long-wave-length oscillations are due to an underlying sharp Fermi surface and disappear when the limit of undoped graphene ($k_F \rightarrow 0$) is approached in pristine graphene.

The above line of research was also extended to the case of

disordered graphene by Lee and coworkers who considered the effect of diagonal and hopping disorder on the RKKY interaction. in undoped [7] and doped graphene [8]. They found that for strong enough on-site disorders where Anderson localization takes place, the RKKY interaction exponentially decays with distance which is consistent with the picture based on localized spectrum [9]. For the doped graphene and weak disorder they found that the Friedel oscillations due to the Fermi surface co-exists with the atomic-scale oscillations due to interference between the two Dirac cones. In this work guided by the experimentally conceivable conditions, instead of a generic Anderson model, we consider a specific model for vacancies and investigate the RKKY interaction in presence of randomly distributed vacancies. Our motivation is that various forms of defects are ubiquitous in the surface of graphene [10]. The presence of defects modifies electronic, magnetic and mechanical properties of materials. For example vacancies generated by ion irradiation of graphene give rise to magnetic moments [11, 12] and the most probable form of defects produced by irradiation are single vacancies [13]. Moreover coherence exchange of spin between such magnetic moments and the spectrum of fermions of the host graphene leads to unconventional Kondo effect in graphene [14, 15].

In this work we find that the randomness caused by random vacancies has a different physics from the Anderson model studied in Ref. [7]: We find that propagation of electron waves in defective environment reduces the exponent α in R^α distance dependence of the RKKY interaction from $\alpha = -3$ to below -4 away from half-filling. The exponent α will not differ from -3 as long as the chemical potential is around energies where the density of states is linear in energy. We find that α is controlled by the concentration of vacancies and the chemical potential, but not much dependent on the energy

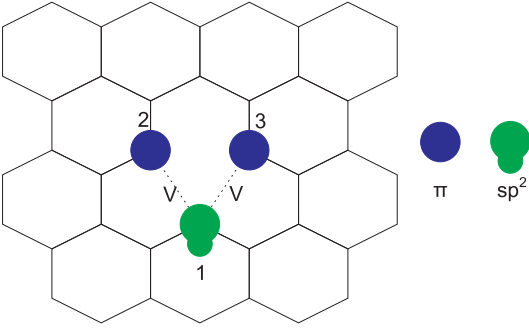


FIG. 1. (Color online) Schematic picture of the electronic state around the defect in graphene. The symbol at site 1 shows the active sp^2 orbital and the circles at sites 2 and 3 the π orbitals. Two of the three sp^2 orbitals ($i = 2, 3$) form a covalent bond. V is the amplitude of the hybridization between the active sp^2 orbital and the two π orbitals.

level of the localized orbitals bound to vacancy location. At higher concentrations of vacancies, they are expected to form their own impurity band, which is expected to cause a metallic type transport in neutral vacancies when the concentration goes beyond a few percent [16, 17]. In such case we expect a Friedel oscillations to appear as a signature of metallic state. But surprisingly we find that in addition to atomic-scale oscillations, the Friedel oscillations of the Fermi surface also disappear.

MODEL AND METHOD

Kanao and coworkers proposed a simple and conceivable model for a localized orbital and its hybridization with the adjacent p_z orbitals needed to understand the physics of local magnetic moments and their interaction with the Dirac electrons of graphene [18]. They considered a Jahn-Teller distorted geometry of a single atom point defect shown in Fig. 1 where the sp^2 orbital of one of the atoms, e.g. 1 is hybridized with p_z orbitals of the two remaining atoms 2, 3 surrounding the vacancy. The effective Hamiltonian for the defective graphene becomes [18] :

$$H = H_g + H_{\text{def}} + H_{\text{hyb}}, \quad (1)$$

where H_g is the tight-binding Hamiltonian of graphene with nearest neighbor hopping and is given by

$$H_g = -t \sum_{\langle ij \rangle \sigma} (a_{i\sigma}^\dagger b_{j\sigma} + \text{h.c.}) - \mu N, \quad (2)$$

where $-t < 0$ is the hopping integral and μ is the chemical potential which can be conveniently controlled by a gate voltage. H_{def} is the effective Hamiltonian for sp^2 orbitals at sites of type 1

$$H_{\text{def}} = \sum_{\sigma} (E_{sp^2} - \mu) d_{\sigma}^\dagger d_{\sigma}, \quad (3)$$

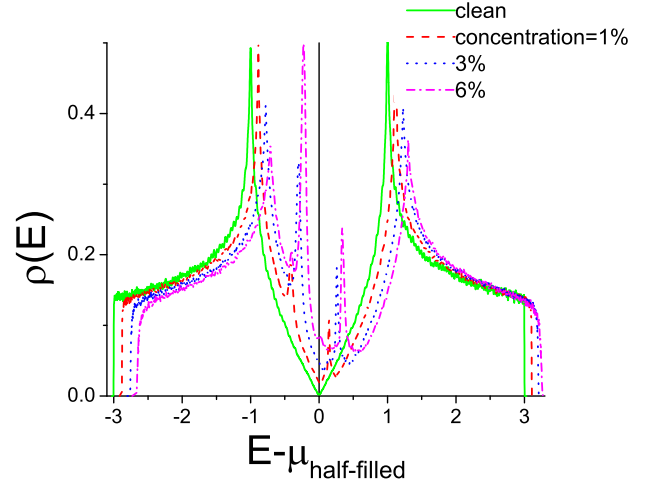


FIG. 2. (Color online) Plot of the density of states $\rho(E)$ as a function of $E - \mu$. By increasing vacancy concentration, $\mu_{\text{half-filled}}$ be shifted to the left of the Dirac neutrality point as the acceptor band to the left of the Dirac point becomes stronger and accommodates more electrons.

where $E_{sp^2} < 0$ is the energy level of the sp^2 orbital and the notation $d_{1\sigma}^\dagger$ is adopted for the creation operator at this site to emphasize its localized nature in analogy with the situation where the localized orbital arises from a transition metal ad-atom. Since in this paper we are interested in the physics of RKKY interaction, we assume that the local moments are formed, and concentrate on their exchange interaction mediated by the electronic states of the defective host. Therefore we do not include the on-site Coulomb repulsion between the electrons in this localized orbital. Finally H_{hyb} is the hybridization which is given for each defect by:

$$H_{\text{hyb}} = V \sum_{\sigma=\uparrow\downarrow} \left[(a_{2\sigma}^\dagger + a_{3\sigma}^\dagger) d_{1\sigma} + \text{h.c.} \right], \quad (4)$$

Here $a_{i\sigma}$ for $i = 2, 3$ is an annihilation operator of a p_z electron at site i with spin $\sigma = \uparrow, \downarrow$ and V is the amplitude of hybridization. The missing carbon atom can belong to both sub-lattices. The Jahn-Teller distortion preferring atom 1 over the other two can take place in any direction. In this paper we take all three possibilities with equal probability. In Eq. 4, we set $V = -0.2t$ for the amplitude of hybridization between p_z and sp^2 orbitals [19] and $E_{sp^2} = -0.5t$, unless otherwise specified.

To have a feeling for what happens to the density of states (DOS) of the vacancy alloyed graphene, in Fig. 2 the DOS of clean honeycomb lattice has been compared to highly vacant graphene. By increasing the concentration of defects, two peaks to the left and right of the Dirac point develop which can be considered as the analogue of bonding and anti-bonding states formed due to the Hybridization term. The chemical potential can be tuned with a gate voltage. In the absence of a gate voltage and for neutral vacancies we have the half-filled situation corresponding to one $2p_z$ electron per existing carbon atom. The chemical potential corresponding to half-

filling deviates to the left of zero when the defects are introduced to the graphene sample. Therefore the $\mu = 0$ in the vacant graphene corresponds to electron doping.

The general perturbative expression for the RKKY exchange interaction is given by [20, 21],

$$J_{\text{RKKY}} = \frac{J^2 S(S+1)}{4\pi S^2} \int d\omega f(\omega) \text{Im} [G(\vec{r}_j, \vec{r}_i, \omega) G(\vec{r}_i, \vec{r}_j, \omega)]$$

where S is the magnitude of the impurity spin, J is the interaction between the localized moments and the spin of the itinerant electrons, i and j are the site index of magnetic impurities which are located at position \vec{r}_i and \vec{r}_j , $f(\omega)$ is the Fermi-Dirac distribution function. Ignoring the constants appearing before the integral, the integral appearing in this equation for our purposes can be simplified to,

$$\Im \int d\omega f(\omega) \sum_{n,m} \frac{F_{nm}^{ij}}{(E_n - \omega + i\delta)(E_m - \omega + i\delta)}. \quad (5)$$

where $F_{nm}^{ij} = \psi_n^*(\vec{r}_i) \psi_n(\vec{r}_j) \psi_m^*(\vec{r}_j) \psi_m(\vec{r}_i)$, with $\psi_n(\vec{r}_i)$ denoting the eigenvector corresponding to the eigenvalue E_n of the host Hamiltonian. The lattice constant a and \hbar are set to unity in all calculations. We assume that temperature is zero ($T = 0$) so that the Lehman representation of the above integral in terms of appropriate spectral functions becomes,

$$J_{\text{RKKY}} = - \int_{\varepsilon < \mu} d\varepsilon \int_{\varepsilon' > \mu} d\varepsilon' \frac{F(\varepsilon, \varepsilon')}{\varepsilon - \varepsilon'}, \quad (6)$$

where $F(\varepsilon, \varepsilon') = \text{Re}[A_{ji}(\varepsilon)A_{ij}(\varepsilon')]$ and the real-space "spectral function" is given by $A_{ij}(\varepsilon) = \langle i | \delta(\varepsilon - H) | j \rangle$. The kernel polynomial method (KPM) can be conveniently used to evaluate various spectral functions including $A_{ij}(\varepsilon)$ [7, 9, 22]. In this method, $A_{ij}(\varepsilon)$ can be expressed as a series in Chebyshev (or any other complete set of orthogonal) polynomials and the expansion coefficients – the so called moments – are evaluated by repeated operation with powers of the appropriate re-scaled Hamiltonian in such a way that a $T_n(H)$ is generated via their recursive relations. In the appendix B we briefly summarize the KPM method. The defects considered here are on the scale of few percent and their positions in the lattice as well as the preferred direction due to Jahn-Teller distortion is drawn from a uniform random distribution. Typical averages are obtained by geometric averages of the form $J_{\text{RKKY}}^{\text{geo}} = \exp(\langle (1/2) \ln(J_{\text{RKKY}})^2 \rangle_{\text{ave}})$. The geometric averages of the above type are known to better represent the propagating nature of waves, and when they become zero indicate the transition to insulating state [7, 8]. To ensure the same holds for our particular form of disorder, in appendix A we have compared the statistics of geometric and arithmetic averages.

NUMERICAL RESULTS FOR THE RKKY EXCHANGE

RKKY interaction in clean graphene

Let us first discuss the performance of KPM in addressing the RKKY interaction. In Ref. 5, the authors used a lattice Green's function method to calculate the RKKY interaction for pristine graphene beyond the low-energy model of Dirac fermions. Their result agrees with other authors [4, 23]. They obtain the following analytical results for the clean honeycomb lattice:

$$J_{\text{AB}}^0 = 3CJ^2 \frac{1 + \cos[\vec{Q} \cdot \vec{R} + \pi - 2\theta_R]}{(R/a)^3} \quad (7)$$

$$J_{\text{AA}}^0 = -CJ^2 \frac{1 + \cos[\vec{Q} \cdot \vec{R}]}{(R/a)^3} \quad (8)$$

where $C = 9\lambda^2 \hbar^2 / (256\pi t)$ is a positive quantity, a is the lattice constant, $\vec{K}^\pm = (\pm 2\pi / (3\sqrt{3}a), 2\pi / (3a))$ are the Dirac points in the momentum space, $\vec{R} = \vec{r}_i - \vec{r}_j$, and angle θ_R is the polar angles between \vec{R} and $\vec{Q} = \vec{K}^+ - \vec{K}^-$. These equations indicating ferromagnetic (antiferromagnetic) correlation on same (different) sub-lattice were numerically confirmed with the KPM method [7, 8]. We have also checked that the KPM results obtained in the clean limit (see Fig. 3) agree with the numerically exact method of Green's functions for the pristine graphene [5, 7]. The strength of the KPM method is that it can handle clean and disordered systems on the same footing. For the disordered case only an averaging over realizations of disorder will be required which is what we explain in detail in the following subsection.

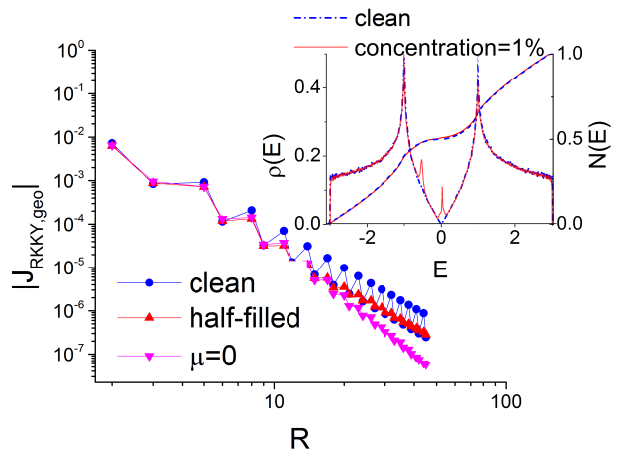


FIG. 3. (Color online) Plot of the J_{RKKY} as a function as R in the armchair direction. By increasing distance R between two magnetic impurities an atomic-scale sign alternation of J_{RKKY} agrees with the analytic formula [5]. For a 1% concentration of vacancies the oscillations due to interference between the two valleys are washed out. The change in the exponent α depends on the chemical potential.

RKKY interactions in heavily vacant graphene

We create evenly distributed defects on the graphene in order to measure their effect on the mediation of RKKY interactions. The energies are measured in units of the hopping amplitude, i.e. we have set $t = 1$. We used a graphene sheet with periodic boundary condition and 2.5×10^5 lattice points are used. We generate 1.5×10^3 different random configurations for the distribution of vacancies. The number of Chebyshev moments is in the range 3000 – 4500. The hybridization parameter is fixed at $V = -0.2t$, and $E_{sp^2} = -0.5t$.

In Fig. 3 we have plotted the distance dependence of the RKKY interaction for a sample with 1% vacancies. The inset shows DOS and the integrated DOS (electron number) for clean and 1% vacant sample. The results are reported for the armchair direction. The first important feature in pristine graphene is the presence of atomic scale oscillations which are due to the interference between two valleys. The second feature which has become more manifest in the log-log plot is that the atomic scale oscillations diminish in long distances for both $\mu_{\text{half-filled}}$ and $\mu = 0$ cases. This means that the Brillouin zone scale wave vector connecting the two Dirac cones of the pristine graphene does not exist in 1% vacant sample anymore.

Another feature seen in the two plots corresponding to vacant sample is that the slope of the exponent α characterizing the overall power-law decay of RKKY interaction stays at $\alpha = -3$ for the half-filled situation, while it is below $\alpha = -3$ for the electron doped ($\mu = 0$) case. To further explore this observation, we check that when the chemical potential falls in the $\rho(E) \propto |E|$ region (which is naturally inherited from the density of states of graphene parent) the exponent remains at $\alpha = -3$ in agreement with other KPM study [8]. Indeed a linear average DOS in two dimensions corresponds to a linear dispersion relation, which by dimensional analysis is expected to give rise to R^{-3} dependence in the particle-hole bubble. This explains why in low concentration regime, despite introducing 1% vacancies, the exponent $\alpha = -3$ in Fig. 3. With this point in mind, we now proceed to study the variations in the exponent α in vacant graphene at $\mu = 0$.

Doping dependence

Based on the discussion in previous subsection, at $\mu = 0$ which corresponds to electron doping in vacant graphene and the chemical potential falls in the region of DOS which is strongly nonlinear, we expect significant variations in the exponent α which can be attributed to hindered motion of electron waves inside the vacant graphene medium. For this, in Fig. 4 we plot the dependence of RKKY interaction to distance in a log-log scale for the armchair direction. To extract the exponent α in the clean and vacant systems, first we discard the length scales below $R = 10a$, as the power-law is meant for long distances. Secondly, slight oscillations surviving the presence of disorder are removed in order to remain

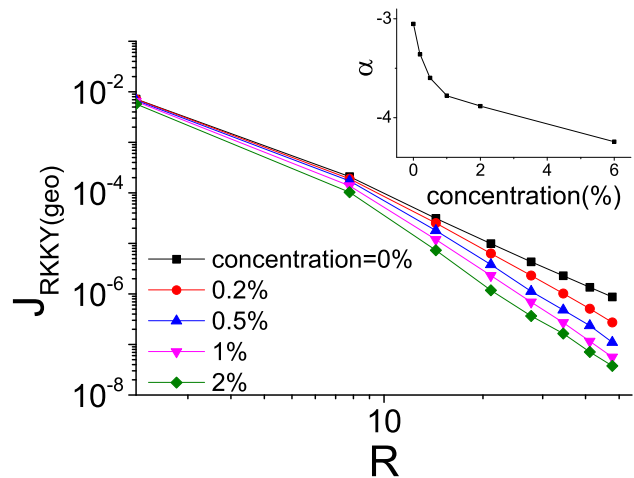


FIG. 4. (Color online) (a) Plot of the J_{RKKY} as a function as R in the electron doped situation ($\mu = 0$). By increasing distance between two magnetic impurities in the armchair direction, J_{RKKY} still decreases with by a power-law. (b) Plot of the α as a function of vacancy concentration in armchair direction. By increasing vacancy concentration, α will decrease. For the zigzag direction the trend is similar, with slightly different exponents at a given concentration.

focused on the power-law part of the dependence. We will return to the question of oscillations in the sequel.

The clear change in the exponent α indicates that the propagation of electrons in heavily vacant graphene is harder than the clean sample which is conceivable as the disorder is expected to make the propagation of both single-particle and particle-hole excitations more difficult. Based on dimensional arguments, the change in α could be effectively ascribed to a change in the average dispersion relation of the electronic states characterizing the vacant sample. Along the zigzag direction a similar conclusion holds, with a minor difference that for a given concentration, the value of the exponent α for the zigzag direction slightly differs from the armchair direction. The qualitative distinction between the armchair and zigzag directions of the pristine graphene does not prevail to the realm of high concentration of vacancies and the qualitative behavior along the two directions are not expected to be much different when a few percent vacancies are introduced.

At the $\mu = 0$ situation we also examine the dependence of α on the energy level E_{sp^2} of the vacancy. As can be seen in Fig. 5 this exponent is not sensitive to the precise value of the impurity level as long as it is not deep enough to allow for the formation of localized bound states which totally changes the nature of propagation of electronic waves.

The fate of Fermi-surface oscillations

When the pristine graphene is doped, in addition to atomic scale oscillations in the RKKY interaction which merely arise from the wave vector \vec{Q} connecting the two Dirac cone val-

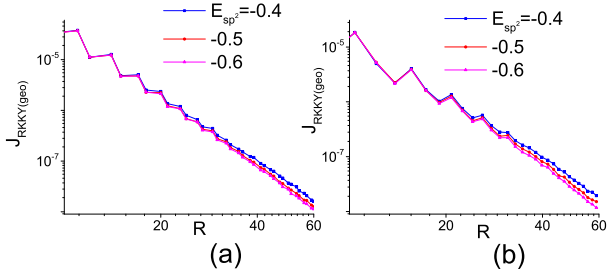


FIG. 5. (Color online) Plot of the J_{RKKY} as a function as distance for (a) armchair and (b) zigzag directions at $\mu = 0$ for different values of E_{sp^2} . As can be seen, the exponent α is not much sensitive to the precise value of E_{sp^2} .

leys, there appears another longer range oscillations due to the presence of extended Fermi surface with characteristic wave-vector k_F [6]. When the disorder is introduced within the Anderson model, both atomic scale oscillations and the Friedel oscillations due to Fermi surface survive [8]. Note that the Dirac picture remains quite robust against the weak disorder [9]. Therefore given the dimensional consistency the overall physics of the RKKY interaction is expected to survive in weak disorders considered in [8]. As we show in the following, for the model of vacant graphene considered here, even the Fermi surface oscillations are washed out. To begin with, note that since the functional dependence of the oscillatory part of the RKKY interaction on distance R always comes through a combination $k_F R$, it could be viewed as an oscillatory function of k_F instead. With this in mind, in Fig. 6 we have plotted the μ -dependence of the pristine and vacant graphene with 1% and 6% vacancies at a fixed distance $R = 32a$. For the clean graphene first of all a perfect particle-hole symmetry is seen in the RKKY interaction which is a symmetry of the Hamiltonian. Secondly an oscillatory depen-

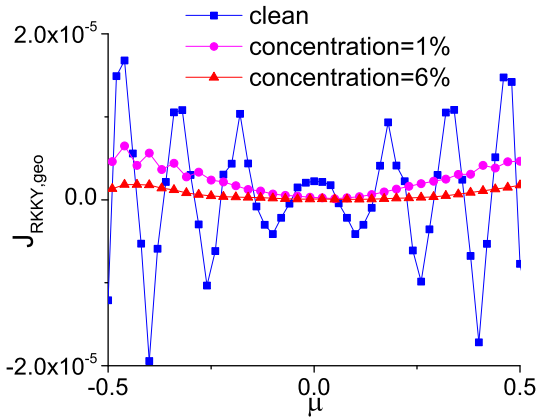


FIG. 6. (Color online) Plot of the J_{RKKY} as a function as μ for armchair direction ($R = 32a$). Vacancies tend to wash out Friedel oscillations. More vacancies do a better job.

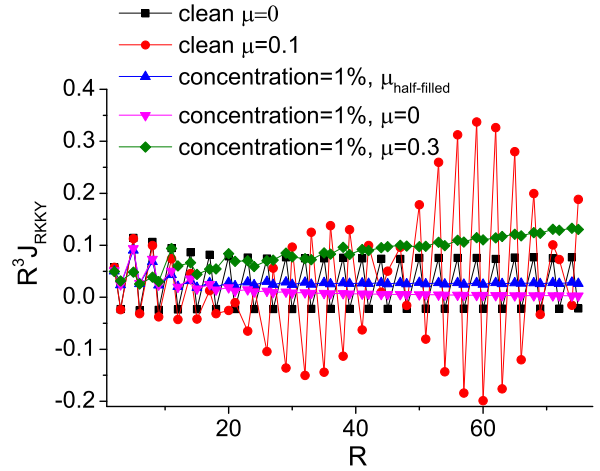


FIG. 7. (Color online) Plot of the $R^3 J_{\text{RKKY}}$ as a function as R for armchair direction. The clean limit is compared with 1% vacancy situation at different doping levels. Adding one percent vacancies kills both type of short-ranged and long-ranged oscillations for the considered chemical potentials.

dence on μ is seen which implies oscillatory dependence on k_F and hence on $k_F R$ on dimensional grounds. By adding vacancies to the system note that the particle-hole symmetry is lost as the presence of vacancies breaks such symmetry. Now at 0.01 vacancy concentration there are no Friedel oscillations up to μ values where the pristine graphene would complete one cycle of oscillations. Some oscillations with reduced amplitude can be seen below the $\mu \approx -0.3$. When the vacancy concentration is increased up to 0.06 no Friedel oscillations can be found.

To compare the real-space profile of the oscillations more clearly, in Fig. 7 we have plotted the $R^3 J_{\text{RKKY}}$ as a function of R along the armchair direction for various values of μ at vacancy concentration 0.01. The plots are contrasted to the case of pristine graphene. As can be seen in the pristine graphene, when the chemical potential is at $\mu = 0$ which corresponds to undoped case, the function $R^3 J_{\text{RKKY}}$ only shows an atomic scale oscillations at large R (black, filled-square plot). When the chemical potential is tuned away from the Dirac point in pristine graphene (the red, filled-circle plot) it can be clearly seen that in addition to the atomic scale oscillations, a Friedel type oscillations due to the presence of a Fermi surface with a definite characteristic scale k_F appear and are superimposed into the atomic scale oscillations in agreement with analytical results for clean graphene [6]. However the striking observation is made when one percent vacancies are introduced. In such case, not only the atomic scale oscillations are diminished, but also no sign of oscillations due to "Fermi surface" are seen at chemical potentials corresponding to half-filling and $\mu = 0.1$. At $\mu = 0.3$ it seems that some tiny atomic scale oscillations are present, while longer range Fermi-surface oscillations are still absent. The absence of Friedel-type oscillations in vacant graphene indicates that

in presence of such amount of vacancies the picture of a Fermi surface with a sharp length scale k_F^{-1} does not hold anymore. It is reminiscent of disorder driven non-Fermi-liquid behavior in Kondo alloys [24] where the creation of vacancies plays a role akin to alloying. Therefore it is likely that in such case the Fermi surface is characterized with multitude of length scales arising from local Fermi surfaces, the disorder averaging over which washes out the part of oscillations corresponding to presence of a sharp single Fermi wave-vector scale of clean metallic state. It should also be noted that in Fig. 7 in the case of pristine graphene the amplitude of long-range oscillations in the function $R^3 J_{\text{RKKY}}$ increases which indicates the decay power in these type of terms is weaker than the R^{-3} behavior [6]. The same argument for the vacant system at $\mu = 0.3$ indicates that the decay power of the J_{RKKY} is not as strong as R^{-3} behavior.

To summarize we find that when vacancies on the scale of a percent are introduced to graphene, the nature of RKKY interaction changes as follows: when the doping level is such that the chemical potential falls in the energy region where DOS is linear, the exponent α in R^α remains at $\alpha = -3$. Otherwise presence of vacancies pushes α to more negative values. Regarding the oscillatory nature of the RKKY interaction in pristine graphene, a few percent vacancies wash out both atomic scale oscillations and the Friedel oscillations due to Fermi surface for a remarkable range of chemical potential values.

ACKNOWLEDGEMENT

SAJ thanks the school of physics, Institute for fundamental research (IPM) for support.

APPENDIX

A: Statistics of geometric averages

In this appendix we present the statistics of our geometric averaging process. We evaluate the probability distributions for both $x = (1/2) \ln(J_{\text{RKKY}}^2)$ (corresponding to geometrical averaging) and J_{RKKY} (corresponding to arithmetic averaging) in Fig. 8 panels (a) and (b) respectively. As can be seen the distribution in x is a Gaussian,

$$P(x) = \frac{N}{\sqrt{2\pi\sigma^2}} \exp\left[-\frac{(x-x_0)^2}{2\sigma^2}\right]. \quad (9)$$

By fitting the Gaussian to the distribution data in panel (a), we find the corresponding width σ of the distribution which as been plotted in Fig. 8 (c) as a function of the impurity concentration. It is interesting to compare the behavior in Fig. 8b with the linear behavior reported in Ref. [8] for a the Anderson model disorder.

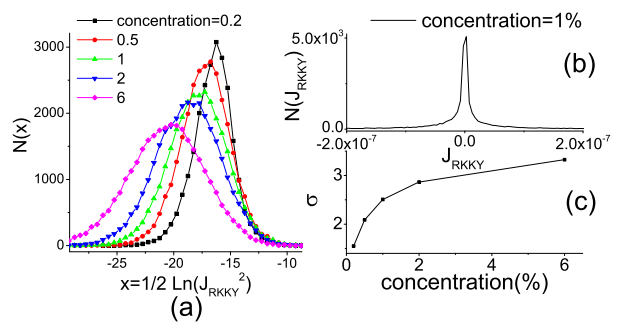


FIG. 8. (Color online). Details of the statistics. (a) The distribution of the quantity $x = (1/2) \ln(J_{\text{RKKY}}^2)$ sampled from the armchair direction distance $R = 60a$. (b) The non-Gaussian distribution of J_{RKKY} (corresponding to arithmetic averaging). (c) Plot of σ in geometric averaging as a function of the percentage of vacancies in armchair direction. By increasing the concentration of vacancies in armchair direction the variance will increase. All data are evaluated for 3×10^4 configurations.

B: Adjusting the chemical potential in KPM

In this appendix we derive a simple relation that enables us to find out the chemical potential corresponding to a given number of electrons in the system. To be self contained, we briefly review the kernel polynomial method (KPM) as well [22].

Consider a quadratic Hamiltonian H whose energy eigenvalues E are limited to a bandwidth $[E_{\text{min}}, E_{\text{max}}]$. Rescaling the Hamiltonian from $H(E)$ to $\hat{H}(\varepsilon)$ where $\hat{H} = (H - b)/a$ and $\varepsilon = (E - b)/a$ where $b = (E_{\text{max}} + E_{\text{min}})/2$ and $a = (E_{\text{max}} - E_{\text{min}})/2$; one can expand spectral functions such as the density of states (DOS) in a complete set of e.g. Chebyshev polynomials defined in the range $\varepsilon \in [-1, 1]$ as,

$$\hat{\rho}(\varepsilon) = \frac{1}{\pi\sqrt{1-\varepsilon^2}} (\mu_0 g_0 + 2 \sum_{m=1}^{N_c} \mu_m g_m T_m(\varepsilon)) \quad (10)$$

where $T_m(\varepsilon) = \cos(m \arccos(\varepsilon))$ are the m th Chebyshev polynomials, μ_m are Chebyshev moments and g_m are appropriate attenuation factors to minimize the Gibbs oscillations. The moments are traces of polynomials of the Hamiltonian and can be statistically calculated as a trace, $\mu_m = 1/r \sum_{r=1}^M \langle \phi_r | T_m(\hat{H}) | \phi_r \rangle$, where ϕ_r are a random single particle states and M is the number of random realizations used in numerical calculations and N_c is a large number where the expansion is cut off. To obtain the effect of $T_m(\hat{H})$ on a given ket, the recurrence relation of Chebyshev polynomials, $T_m(\hat{H}) = 2\hat{H}T_{m-1}(\hat{H}) - T_{m-2}(\hat{H})$ with initial conditions $T_1(\hat{H}) = \hat{H}$ and $T_0(\hat{H}) = 1$ are used. At the end the DOS in the original bandwidth scale is obtained as $\rho(E) = \hat{\rho}(\varepsilon)/a$.

The spectral functions corresponding to space non-diagonal propagation can also be similarly calculated between any two points i and j in the lattice,

$$\hat{\rho}_{ij}(\varepsilon) = \frac{1}{\pi\sqrt{1-\varepsilon^2}} (\mu_0^{ij} g_0 + 2 \sum_{m=1}^M \mu_m^{ij} g_m T_m(\varepsilon)) \quad (11)$$

where the non-local moment μ_m^{ij} is given by the matrix element $\langle i|T_m(\hat{H})|j\rangle$.

When we add vacancies in a graphene sheet, the particle-hole symmetry is lost, and the half-filling will not correspond to $\mu = 0$ anymore. Therefore within the KPM we need to find a formula to give a relation between the particle number density n and the chemical potential μ . The filling factor is given by,

$$n(\mu) = \int_{-1}^{+1} \theta(\varepsilon - \mu) \hat{\rho}(\varepsilon) d\varepsilon \quad (12)$$

where $\theta(\varepsilon - \mu)$ is Heaviside function and μ is the (scaled) Fermi level. Expanding the integral in Chebyshev polynomials and using the trigonometric representation of Chebyshev polynomials one can easily perform the integration to get,

$$n = \frac{\mu_0 g_0}{\pi} \arccos(-\mu) - 2 \sum_{m=1}^{N_c} \frac{\mu_m g_m}{m\pi} \sin(m \arccos \mu) \quad (13)$$

For a given n one needs to adjust μ to satisfy this equation. Then the physical μ is obtained by undoing the rescaling. For example it can be checked that in clean graphene, the solution of the above equation with $n(\mu) = 0.5$ will be $\mu = 0$.

-
- [1] K. S. Novoselov, A. K. Geim, S. V. Morozov, D. Jiang, Y. Zhang, S. V. Dubonos, I. V. Grigorieva, and A. A. Firsov, *Science* **306** (2004) 666.
 [2] For a concise review, see e.g. T. Ando, *Physica E*, **40** (2007) 213.
 [3] M. I. Katsnelson, *Materials Today*, **10** (2007) 20.

- [4] S. Saremi, *Phys. Rev. B* **76** (2007) 184430.
 [5] M. Sherafati and S. Satpathy, *Phys. Rev. B* **83** (2011) 165425.
 [6] M. Sherafati and S. Satpathy, *Phys. Rev. B* **84** (2011) 125416.
 [7] H. Lee, J. Kim, E. R. Mucciolo, G. Bouzerar and S. Kettemann, *Phys. Rev. B* **85** (2012) 075420.
 [8] H. Lee, J. Kim, E. R. Mucciolo, G. Bouzerar and S. Kettemann, *Phys. Rev. B* **86** (2012) 205427.
 [9] M. Amini, S. A. Jafari, F. Shahbazi, *Eur. Phys. Lett.* **87** (2009) 37002.
 [10] A. Hashimoto, K. Suenaga, A. Gloter, K. Urita and S. Iijima, *Nature* **430** (2004) 870.
 [11] R. R. Nair, M. Sepioni, I-Ling Tsai, O. Lehtinen, J. Keinonen, A. V. Krasheninnikov, T. Thomson, A. K. Geim and I. V. Grigorieva, *Nature Phys.* **8** (2012) 199.
 [12] O. Yazyev, L. Helm, *Phys. Rev. B* **75** (2007) 125408.
 [13] M. M. Ugeda, I. Brihuega, F. Guinea, and J. M. Gomez-Rodriguez, *Phys. Rev. Lett.* **104** (2010) 096804.
 [14] J-H. Chen, W. G. Cullen, C. Jang, M. S. Fuhrer, and E. D. Williams, *Phys. Rev. Lett.* **102** (2009) 236805.
 [15] J.-H. Chen, W. G. Cullen, E. D. Williams, and M. S. Fuhrer, *Nature Phys.* **7** (2011) 535.
 [16] D. Haberer et al., *Phys. Rev. B* **83** (2011) 165433.
 [17] M. Allaei, S. A. Jafari, H. Akbarzadeh, *J. Phys. Chem. Solids*, **69** (2008) 3283.
 [18] T. Kanao, H. Matsuura, and M. Ogata, *J. Phys. Soc. Jpn.* **81** (2012) 063709.
 [19] D. Porezag, Th. Frauenheim, Th. Khler, G. Seifert, and R. Kaschner, *Phys. Rev. B* **51**, 12947 (1995).
 [20] J. Sólyom, *Fundamentals of the physics of solids*, Vol. 3, Springer, Berlin (2010).
 [21] R. M. White, *Quantum Theory of Magnetism* McGraw-Hill, New York, (1970).
 [22] A. Weiße, G. Wellein, A. Alvermann, and G. Fehske, *Rev. Mod. Phys.* **78** (2006) 275.
 [23] M. Black-Schaffer, *Phys. Rev. B* **81** (2010) 205416.
 [24] E. Miranda, V. Dobrosavljevic and G. Kotliar, *Phys. Rev. Lett.* **78** (1997) 290.